

## Surface-Mediated Growth of Transparent, Oriented, and Well-Defined Nanocrystalline Anatase Titania Films

Donghai Wang,<sup>†</sup> Jun Liu,<sup>\*,†</sup> Qisheng Huo,<sup>†</sup> Zimin Nie,<sup>†</sup> Weigang Lu,<sup>†</sup> Rick E. Williford,<sup>†</sup> and Ying-Bing Jiang<sup>‡</sup>

*Pacific Northwest National Laboratory, Richland, Washington 99352, and University of New Mexico, Albuquerque, New Mexico 87131*

Received August 2, 2006; E-mail: jun.liu@pnl.gov

Numerous chemical and physical methods have been investigated for preparing anatase TiO<sub>2</sub> films owing to their important electronic, optical, and catalytic properties. Among these, chemical methods (sol-gel synthesis<sup>1,2</sup> and solution deposition<sup>3</sup>) are of particular interest because of the simplicity and wide applicability. However, up to date, chemical synthesis of oriented transparent anatase films with well-defined crystallinity and morphology has not been reported. Literature results strongly suggest that in TiO<sub>2</sub> the electrochemical<sup>4,5</sup> and catalytic properties<sup>6</sup> and the energy conversion efficiency in photovoltaics<sup>7</sup> depend on specific surfaces and growth orientation. Even though anatase is believed to be catalytically more active, fundamental understanding of the surface chemistry of this important material falls far behind that of the rutile phase because of the difficulty to obtain quality crystals.<sup>8</sup> The ability to prepare oriented, well-defined nanocrystalline anatase films would provide new opportunities to study the orientation and structure dependent properties and optimize the device performance.

In this paper we explore a powerful technique using functionalized surface to assist anatase film growth. This method has been applied to iron oxide,<sup>9</sup> calcium carbonate,<sup>10</sup> zinc oxide,<sup>11</sup> etc. Similar efforts to make TiO<sub>2</sub> produced films with poor control of crystallinity and morphology<sup>12</sup> or films with packed, ultrafine crystallites,<sup>13</sup> likely due to the difficulty in controlling the solubility. The success of our approach depends on the slow hydrolysis and oxidation of the titanium trichloride precursor (Figure S1)<sup>14,15</sup> and on the appropriate choice of the functional molecules on the substrate and the solution chemistry.

Glass substrates functionalized with different terminal groups, such as -NH<sub>2</sub>, -SO<sub>3</sub>H, -COOH, and -OH functionalized substrates, were used to grow anatase TiO<sub>2</sub>.<sup>15</sup> Oriented and well-defined nanocrystalline TiO<sub>2</sub> films are obtained on amine (-NH<sub>2</sub>) functionalized surfaces (Figure 1a). The film is made of octahedron-shaped anatase nanocrystals bounded by eight triangular surfaces, approximately 90–150 nm wide. The inset in Figure 1a shows a high-magnification image of typical octahedral bipyramidal nanocrystals formed on bare glass substrates under the same experimental conditions. The TiO<sub>2</sub> films are continuous and quite transparent in the visible range (Figure 1b and Figure S2<sup>15</sup>). On -COOH (Figure 1c) and other surfaces (Figure S3<sup>15</sup>), agglomerated crystals or noncontinuous films were observed.

Figure 1d and Figure 1e show a tilted view scanning electron microscopy (SEM) image and a 3 μm × 3 μm atomic force microscope (AFM) image, respectively, revealing that the TiO<sub>2</sub> nanocrystals have preferred orientation with most of their tips roughly pointing upward, suggesting that the [001]-axis may be oriented perpendicular to the substrate.

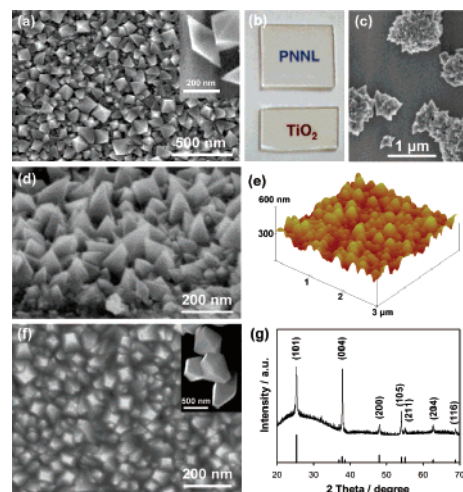


**Figure 1.** (a) A top-view SEM image of an octahedral nanocrystalline TiO<sub>2</sub> film (200 nm thick) on amine functionalized glasses. The inset shows octahedral bipyramidal crystals grown on bare glasses. (b) Photograph of an octahedral pyramidal nanocrystalline TiO<sub>2</sub> film in 200 nm (up) and 100 nm (bottom) thicknesses on amine functionalized glasses.<sup>15</sup> (c) Top-view SEM image of agglomerated TiO<sub>2</sub> nanocrystals grown on -COOH functionalized glasses. (d) SEM image of the 60°-tilted sample in panel a. (e) AFM image of the sample in panel a. (f) Top-view SEM image of a TiO<sub>2</sub> film (200 nm thick) on amine functionalized substrates composed of oriented truncate octahedral nanocrystals prepared using ethylene glycol/water solution (1:5 mixture) as solvent.<sup>15</sup> The inset shows truncate octahedral bipyramidal crystals grown on bare glasses. (g) XRD pattern of the sample in panel f at  $\theta$ - $2\theta$  scan and the expected peak positions for anatase.

The morphology of the nanocrystals can be finely tuned. The introduction of alcohol in the solution under similar synthesis conditions produced TiO<sub>2</sub> films with oriented, truncate octahedral pyramidal nanocrystals (Figure 1f)<sup>15</sup> that are close to the equilibrium shape of anatase crystals.<sup>16</sup> Smooth (001) square top planes are clearly observed. The X-ray diffraction (XRD,  $\theta$ - $2\theta$  scan) pattern of the TiO<sub>2</sub> film confirms crystalline anatase phase (JCPDS No. 21-1272). Moreover, significantly enhanced peaks of both (004) and (105) reflections further confirm a preferred [001]-oriented anatase TiO<sub>2</sub> film perpendicular to the substrate.

Figure 2a shows a cross-sectional transmission electron microscope (TEM) image of the nanocrystalline film. The TiO<sub>2</sub> film is composed of oriented octahedral pyramidal nanocrystals with smooth side surfaces. A high-resolution TEM (HRTEM) image of an octahedral pyramidal nanocrystal (Figure 2b) shows crystalline lattice fringes which are parallel to the side surface of the octahedron. The measured distance (3.5 Å) between the adjacent lattice fringes can be assigned to the interplanar distance (3.52 Å) of anatase TiO<sub>2</sub> (101) planes. The [101] zone axis is then perpendicular to the side surface of the octahedral pyramidal nanocrystal. Most of the octahedral pyramidal nanocrystals in the

<sup>†</sup> Pacific Northwest National Laboratory.

<sup>‡</sup> University of New Mexico.

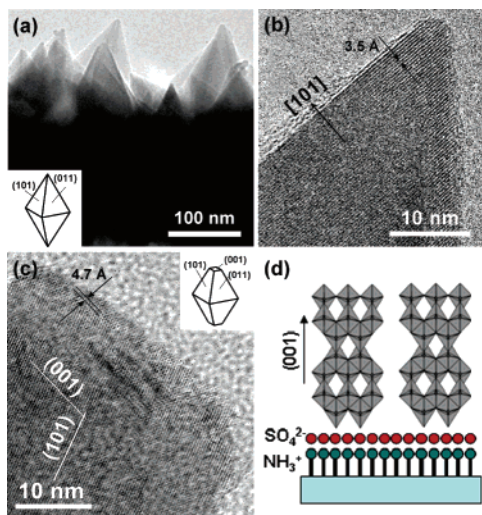


**Figure 2.** (a) A cross-sectional TEM image of an octahedral pyramidal nanocrystalline TiO<sub>2</sub> film (200 nm thick); (inset) a schematic drawing of an octahedral bipyramid. (b) HRTEM image of an octahedral pyramidal nanocrystal; (inset) schematic drawing of a truncate octahedral bipyramid. (c) HRTEM image of a truncate octahedral pyramidal nanocrystal in that film with truncate surface, 35 nm in width. The image reveals two sets of crossing lattice fringes. The angle between the crossing fringes is 112°. The lattice fringes (3.5 Å spacing) parallel to the side surface are assigned to (101) planes, while the other crossing fringes (4.7 Å spacing) parallel to the top surface are assigned to (002) planes. The truncate octahedral pyramidal nanocrystals are consistent with the equilibrium shape of anatase TiO<sub>2</sub> crystals, that is, truncate octahedral bipyramid as illustrated in the inset of Figure 2c. (d) Illustration of surface-mediated growth of oriented anatase TiO<sub>2</sub> nanocrystals.

TiO<sub>2</sub> film have sharp tops and are only slightly rounded in the high resolution (HRTEM) image, conforming to the shape of an octahedral bipyramid bounded by eight triangular crystalline planes (inset in Figure 2a). A cross-sectional TEM image (Figure S4)<sup>15</sup> confirms another TiO<sub>2</sub> film composed of oriented, truncate octahedral pyramidal TiO<sub>2</sub> nanocrystals. Figure 2c shows a HRTEM image of a truncate octahedral pyramidal nanocrystal in that film with truncate surface, 35 nm in width. The image reveals two sets of crossing lattice fringes. The angle between the crossing fringes is 112°. The lattice fringes (3.5 Å spacing) parallel to the side surface are assigned to (101) planes, while the other crossing fringes (4.7 Å spacing) parallel to the top surface are assigned to (002) planes. The truncate octahedral pyramidal nanocrystals are consistent with the equilibrium shape of anatase TiO<sub>2</sub> crystals, that is, truncate octahedral bipyramid as illustrated in the inset of Figure 2c.

The continuous, transparent, and oriented nanocrystalline film is a direct result of the surface-mediated nucleation process. Under our experimental condition (pH = 1~2),<sup>15</sup> the amine terminated groups on the substrate are positively charged.<sup>17</sup> Thus negatively charged SO<sub>4</sub><sup>2-</sup> ions should be preferentially attracted to the -NH<sub>2</sub> substrate. These SO<sub>4</sub><sup>2-</sup> ions likely serve as the nucleation sites for the anatase crystals (Figure 2d).<sup>18,19</sup> Based on the titanyl sulfate structure, the sulfate tetrahedra prefer binding to the vertexes of the Ti-O octahedra.<sup>20,21</sup> The anatase (001) plane contains edge-sharing octahedra with the highest density of vertexes to bind to the sulfate ions on this plane. This may explain the origin of the [001] orientation in the TiO<sub>2</sub> films. The orientation may also be a result of grain boundary motion during film growth<sup>22</sup> or kinetic anisotropic crystal growth in which the fast growth orientation prevails.<sup>13,23</sup> Other groups (-SO<sub>3</sub>H, -COOH, and -OH) are not highly charged at the low pH values,<sup>17</sup> and therefore do not provide the electrostatic attraction mentioned earlier for the crystal growth. However, the role of functional groups on crystal growth is quite complex and is under intense study from many groups.<sup>10</sup>

In our experiments, well-defined octahedral pyramidal nanocrystals were only observed when poly(vinylpyrrolidone) (PVP) was used in the solution. PVP is widely used for shape-controlled nanoparticle synthesis owing to preferred adsorption on specific surfaces.<sup>24</sup> Our results suggest that the preferred adsorption of PVP may be on the (101) anatase surface, resulting in (101)-plane-dominated octahedral bipyramids. When ethylene glycol or other alcohol is introduced, it may function as cosolvent and reduce the tendency for PVP to adsorb onto the surface.<sup>25</sup> Thus the crystals have a chance to evolve into the typical equilibrium shape, that is, truncate octahedral bipyramids.<sup>16</sup> The degree of truncation increases with increasing the amount of alcohol (Figure S5).<sup>15</sup>

In summary, we developed a new, surface-mediated method to grow transparent and oriented anatase TiO<sub>2</sub> films with tunable, well-defined nanocrystalline morphologies. This combination of desirable properties is important for studying the structure-dependent physical and chemical properties, and for improving the performance of the material and devices.

**Acknowledgment.** The work is supported by PNNL's Laboratory-Directed Research and Development Program and by the Office of Science (DOE). PNNL is a multiprogram laboratory operated by Battelle Memorial Institute for the Department of Energy under Contract DE-AC06-76RLO1830.

**Supporting Information Available:** Experimental procedure and characterization (Figure S1–S6). This material is available free of charge via the Internet at <http://pubs.acs.org>.

## References

- (1) Negishi, N.; Iyoda, T.; Hashimoto, K.; Fujishima, A. *Chem. Lett.* **1995**, 841–842.
- (2) Takahashi, Y.; Matsuoka, Y. *J. Mater. Sci.* **1988**, *23*, 2259–2266.
- (3) Niesen, T. P.; De Guire, M. R. *J. Electroceram.* **2001**, *6*, 169–207.
- (4) Hengerer, R.; Kavan, L.; Krtil, P.; Gratzel, M. *J. Electrochem. Soc.* **2000**, *147*, 1467–1472.
- (5) Kavan, L.; Gratzel, M.; Gilbert, S. E.; Klemenz, C.; Scheel, H. J. *J. Am. Chem. Soc.* **1996**, *118*, 6716–6723.
- (6) Linsebigler, A. L.; Lu, G. Q.; Yates, J. T. *Chem. Rev.* **1995**, *95*, 735–758.
- (7) Deng, H. H.; Zhang, H.; Lu, Z. H. *Chem. Phys. Lett.* **2002**, *363*, 509–514.
- (8) Diebold, U. *Surf. Sci. Reports* **2003**, *48*, 53–229.
- (9) Bunker, B. C.; Rieke, P. C.; Tarasevich, B. J.; Campbell, A. A.; Fryxell, G. E.; Graff, G. L.; Song, L.; Liu, J.; Virden, J. W.; McVay, G. L. *Science* **1994**, *264*, 48–55.
- (10) Aizenberg, J.; Black, A. J.; Whitesides, G. H. *J. Am. Chem. Soc.* **1999**, *121*, 4500–4509.
- (11) Hsu, J. W. P.; Tian, Z. R.; Simmons, N. C.; Matzke, C. M.; Voigt, J. A.; Liu, J. *Nano Lett.* **2005**, *5*, 83–86.
- (12) (a) Shin, H.; Collins, R. J.; Deguire, M. R.; Heuer, A. H.; Sukenik, C. N. *J. Mater. Res.* **1995**, *10*, 692–698. (b) Baskaran, S.; Song, L.; Liu, J.; Chen, Y. L.; Graff, G. L. *J. Am. Ceram. Soc.* **1998**, *81*, 401–408.
- (13) Masuda, Y.; Sugiyama, T.; Seo, W. S.; Koumoto, K. *Chem. Mater.* **2003**, *15*, 2469–2476.
- (14) Hosono, E.; Fujihara, S.; Kakiuchi, K.; Imai, H. *J. Am. Chem. Soc.* **2004**, *126*, 7790–7791.
- (15) See Supporting Information for additional details and data.
- (16) Lazzeri, M.; Vittadini, A.; Selloni, A. *Phys. Rev. B: Condens. Matter Mater. Phys.* **2001**, *63*, 15.
- (17) Shyue, J. J.; De Guire, M. R. *Langmuir* **2004**, *20*, 8693–8698.
- (18) Li, Y. Z.; Lee, N. H.; Hwang, D. S.; Song, J. S.; Lee, E. G.; Kim, S. J. *Langmuir* **2004**, *20*, 10838–10844.
- (19) Yamabi, S.; Imai, H. *Chem. Mater.* **2002**, *14*, 609–614.
- (20) Bokhimi, X.; Morales, A.; Ortiz, E.; Lopez, T.; Gomez, R.; Navarrete, J. *J. Sol-Gel Sci. Technol.* **2004**, *29*, 31–40.
- (21) Gatehouse, B. M.; Platts, S. N.; Williams, T. B. *Acta Crystallogr., Sect. B: Struct. Sci.* **1993**, *49*, 428–435.
- (22) Thompson, C. V. *Annu. Rev. Mater. Sci.* **2000**, *30*, 159–190.
- (23) Tian, Z. R.; Voigt, J. A.; Liu, J.; McKenzie, B.; McDermott, M. J.; Rodriguez, M. A.; Konishi, H.; Xu, H. F. *Nat. Mater.* **2003**, *2*, 821–826.
- (24) Wiley, B.; Sun, Y. G.; Mayers, B.; Xia, Y. N. *Chem.-Eur. J.* **2005**, *11*, 454–463.
- (25) Benalla, H.; Zajac, J. J. *Colloid Interface Sci.* **2004**, *272*, 253–261.

JA0655993